Studies of Indoor Wave Propagation and Antenna Diversity in UHF RFID Systems

Luis Carlos Vieira, Nathan J. Gomes, John C. Batchelor, Philippos Assimakopoulos, and Lucas D. Schwendler Vieira

***Abstract*—Analytical and experimental investigations considering indoor wave propagation and antenna diversity are presented for passive UHF RFID systems. Modelling results are reported for two-ray and three-ray reflection models, with the effect of floor and ceiling relative permittivity discussed. A novel multi-LOS multi-ray reflection model, considering transmit antenna diversity, is proposed with good results reported. From experiments, a receive diversity scheme shown the best performance in comparison with transmit diversity and no diversity cases. A promising performance improvement in the tag readability is also demonstrated (without antenna diversity) by simply placing an aluminium plate on the floor nearby a commercial tag.**

Keywords — RFID; antenna diversity; indoor propagation modelling.

I. INTRODUCTION

Ultra-high frequency (UHF) radio frequency identification (RFID) systems have many potential applications, such as asset tracking, supply chain management, and Internet of Things (IoT). UHF RFID is a radio transponder backscatter system that generally comprises active readers and tags. The tags modulate onto the backscattered signals their unique identify codes, together with other relevant information. RFID tags may be active, battery assisted and passive depending on applications [1].

In passive UHF RFID systems, high transmit power is needed as the passive tags are powered from the reader's transmitted RF signal. However, leakage of the transmit power into the reader's receiver input may saturate amplifiers and analog-to-digital converters (ADCs). Thus, high isolation between the transmit and receive RFID channels is required.

In [2], a distributed antenna UHF RFID system using antenna diversity in conjunction with phase and frequency hopping was proposed for enhancing tag detection performance. Good system performance was demonstrated using less RFID readers than for a conventional RFID system. However, the proposed technique imposes a limit on tag read speed due to the required number of phase and frequency steps. In addition, high antenna separation is needed for the technique work well [2]. In [3], the implementation of maximal ratio combining (MRC) on a dual antenna diversity receiver platform for RFID was presented. Although the proposed scheme outperforms the conventional antenna switching technique, it requires the duplication of the reader receive frontend and increases signal processing complexity.

The wireless indoor propagation between a transmitter and receiver is usually unstable due to multipath effects, these effects caused by the constructive/destructive interference between the main (direct) signal and the reflected signals from any fixed objects like walls, tables, and any moving objects. The Friis free space model [4] is used in some RFID researches to represent the wave propagation, e.g. [5] [6]. However, this model does not hold for short distances (in the order of the RF carrier wavelength) and does not consider multipath fading. Ray tracing is commonly used to model multipath propagation in both indoor and outdoor scenarios and have been used in some RFID studies [7] [8].

In this work, we study the RFID system performance considering spatial antenna diversity and indoor wave reflection. The authors have previously reported RFID experiments with similar antenna diversity schemes considering, however, the transmission of RFID signals through a multimode fiber (MMF) link [9]. In the work now reported, no MMF link is used. A ray-tracing based model is described and used to analyze the indoor propagation at a UHF RFID frequency and considering the ceiling and floor reflections. In addition, a novel propagation model for multiple transmit antenna and multi-ray reflection scenario is proposed. Previous works have considered the design of RFID tags mounted on top of a metallic ground plane [10-12]. In this work, however, no specific tag is designed and fabricated and good performance results are achieved by just using a commercial tag and a rectangular aluminum plate placed on the floor in front of the tag. To the best of the authors' knowledge, no previous demonstration has been reported using similar tag-metallic plate configuration.

II. ANALYSIS OF INDOOR MULTIPATH PROPAGATION

In this section, we initially describe an analytical propagation model for indoor multipath environments considering up to three propagation paths. We discuss the effect of indoor reflection on the received power level in comparison with free space propagation. In addition, a new multipath propagation model considering transmit antenna diversity is introduced. Modelling results are presented for the two-ray and three-ray models, and for the proposed model with four propagation paths.

The received power at the RFID tag in a multipath environment with several reflected ray paths can be modelled as [13]

$$P_{tag} = kP_t\left(\frac{\lambda}{4\pi}\right)^2\left|\frac{\sqrt{G_{los}}}{d_{los}}+\sum_{n=1}^{N}\frac{R_n\sqrt{G_n}\,e^{jk(d_n-d_{los})}}{d_n}\right|^2 \quad (1)$$

where P_t is the transmitted power, d_{los} is the length of the direct line-of-sight (LOS) path, d_n is the length of the n-th reflected

Luis C. Vieira, UTFPR, Curitiba, Brazil, e-mail: vieira@utfpr.edu.br; Nathan J. Gomes, John C. Batchelor, and Philippos Assimakopoulos are with the University of Kent, UK, e-mails: N.J.Gomes@kent.ac.uk, J.C.Batchelor@kent.ac.uk, P.Asimakopoulos@kent.ac.uk; Lucas D. Schwendler Vieira, Curitiba, Brazil, e-mail: lucas.dsv@hotmail.com. This work was partially supported by the Newton Research Collaboration Programme – Royal Academy of Engineering (NRCP1516/1/139).

ray path, G_{los} and G_n are the product of the reader and tag antenna gains in the LOS and the n-th ray directions, λ is the wavelength of the carrier frequency, and k=2π/λ is the wavenumber. We have included the loss factor k in (1) to account for other system losses such as impedance mismatch between the tag antenna and tag chip. R_n is the n-th reflection coefficient that depends on the relative permittivity ε_r of the reflecting object and the incidence angle θ. The reflection coefficient for horizontal polarization can be calculated as [4]

$$R_n = \frac{\sin\theta - \sqrt{\varepsilon_r - \cos^2\theta}}{\sin\theta + \sqrt{\varepsilon_r - \cos^2\theta}} \quad (2)$$

If just the floor reflection is considered $N = 1$ and (1) becomes the classical two-ray ground reflection model. Using the notations in Fig. 1, $d_{los} = \sqrt{d^2 + (h_{rd} - h_{tag})^2}$, and the length of the floor reflected ray path is $d_1 = \sqrt{d^2 + (h_{rd} + h_{tag})^2}$. The floor reflection coefficient R_1 is given by (2), with $\sin\theta_1 = (h_{rd} + h_{tag})/d_1$ and $\cos\theta_1 = d/d_1$.

In this work, our three-ray model includes the floor and ceiling reflections. From geometrical derivation and for a ceiling height h_c, the length of the ceiling reflection path is $d_2 = \sqrt{d^2 + (2h_c - h_{rd} - h_{tag})^2}$ and the coefficient R_2 is calculated by (2) with $\sin\theta_2 = (2h_c - h_{rd} - h_{tag})/d_2$ and $\cos\theta_2 = d/d_2$.

Now, we introduce a modification of (1) to also consider the interference amongst the LOS rays from multiple transmit antennas with same power level in-phase signals as inputs. For the ray-propagation diagram of Fig. 1, the difference now is that there are additional reader antennas placed in different positions. We have named the new model as multi-LOS multi-ray reflection model. The electric field at the received antenna is the result of the superposition of all direct LOS rays and reflected rays. Thus, the received power at the tag is given by

$$P_{tag} = kP_t\left(\frac{\lambda}{4\pi}\right)^2 \left| \sum_{i=1}^{M} \frac{\sqrt{G_{los,i}}}{d_{los,i}} e^{jkd_{los,i}} + \sum_{n=1}^{N} \frac{R_n\sqrt{G_n}\, e^{jkd_n}}{d_n} \right|^2 \quad (3)$$

where $G_{los,i}$ is the product of the reader and tag antenna gains in the i-th LOS ray directions, d_n is the length of the n-th reflected ray path (originated from any antenna), and $d_{los,i}$ is the length of the i-th LOS path given by

$$d_{los,i} = \sqrt{d^2 + (h_{rd,i} - h_{tag})^2} \quad , i = 1, \ldots M. \quad (4)$$

The modelled results for both the two-ray and three-ray models are shown in Fig. 2. The modelling parameters are presented in Table I. These values were chosen to be the same as those of the experiment reported in Section IV-B.

From Figs. 2a and 2b, the simulation results show that the indoor reflections increase the power level in comparison with the free space for the distances in between 2 and around 10 m, for the two-ray model. The variations in the power level are better modelled using the three-ray model in comparison with the two-ray one. When the floor relative permittivity is increased from 2 (Fig. 2a) to 12 (Fig. 2b) it can be seen that the power levels of the reflection models also increase. Considering a tag sensitivity of -20 dBm (the same as that of the tag used in our experiments) the reading range is around 7 m for the three-ray model results in Figs. 2a and 2b. In free space the reading range is approximately 5.5 m. By comparing the results from Figs. 2b and 2c, it can be seen that the degree of the power level fluctuations increases when the ceiling relative permittivity is increased from 3 to 10. From Fig. 2c, we can see that the reading range could even achieve 9 m for a tag sensitivity of -20 dBm if a high reflective material, with e.g. ε_r = 10, is used in the ceiling.

The modelling results using the proposed multi-LOS multi-ray reflection model are shown in Fig. 3. They are obtained for two transmit antenna diversity (M = 2) and up to two ground reflected rays (N = 2) in (3), and for P_t = +18.2 dBm, $h_{rd,1} = h_{tag}$ = 1.23 m, $h_{rd,2}$ = 0.85 m, ε_{rf} = 2. These values are the same as those of the 2Tx-1Rx experiment reported in Section IV-A The other modelling parameters are shown in Table I. We note that, for all modelling cases, the antenna gains are adjusted as a function of the angle between the i-th LOS direction or the n-th reflected ray direction and the horizontal plane.

The shape of the 2Tx diversity, 2 reflected ray result in Fig. 3 resembles that of the 2Tx-1Rx measured result in Fig. 6. However, it can be observed that the attenuation from 0.8-m to 2.5-m distance is around 7 dB and 15 dB in Figs. 3 and 6, respectively. This is because only the reader-to-tag attenuation is considered in the model of (3) while the total RFID link attenuation is shown in Fig. 6. Higher power levels are obtained for the modelling results of Fig. 3 in comparison with those of Fig.2. This is due to the higher tag height and also the antenna diversity effect considered in the results of Fig.3.

TABLE I. *MODELLING PARAMETERS.*

Parameter	Value
Frequency (f)	865.7 MHz
Transmitted power (P_t)	+21.2 dBm
Loss factor (k)	0.8
Reader antenna height (hrd)	1.23 m
Tag height (htag)	0.265 m
Ceiling height (hc)	3.19 m
Tag antenna gain (Gtag)	0 dBi (max.)
Reader antenna gain (Grd)	6 dBi (max.)
Floor relative permittivity (ε_{rf})	2 and 12
Ceiling relative permittivity (ε_{rc})	3 and 10

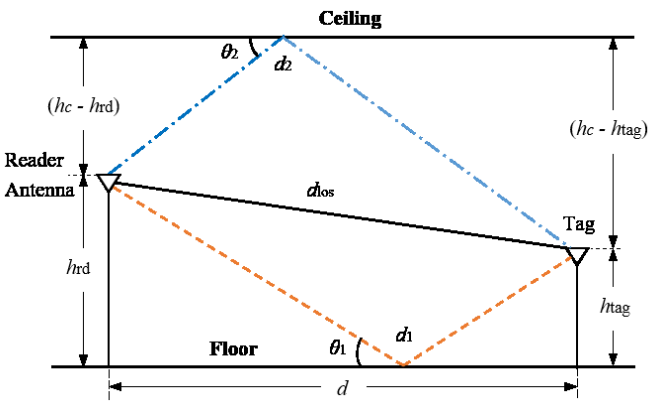

Fig. 1. Ray-propagation diagram.

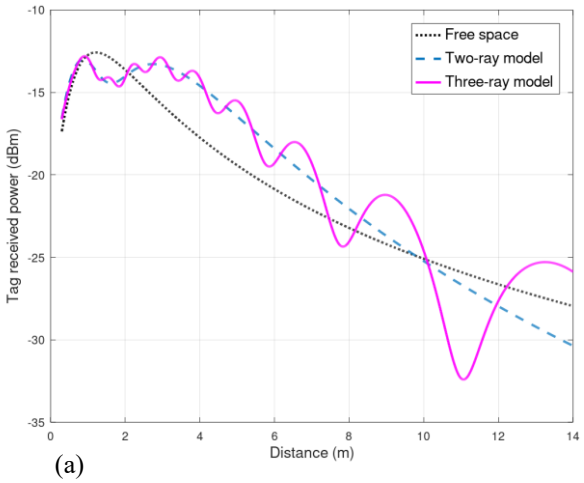

(a)

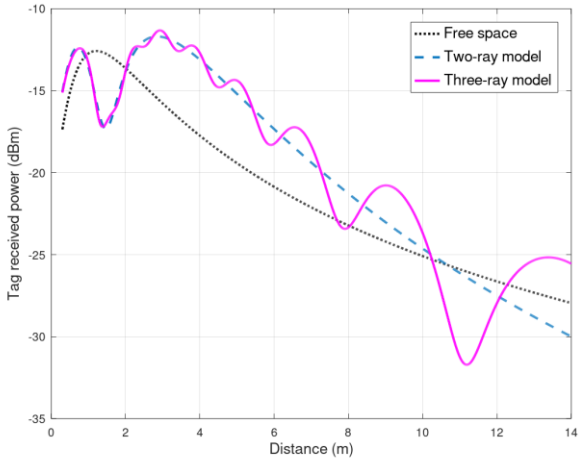

(b)

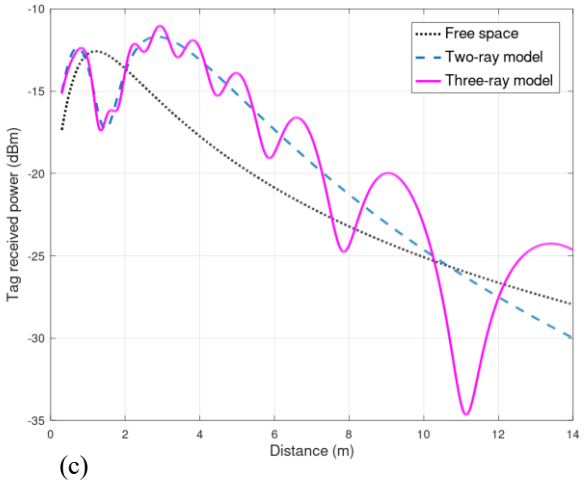

(c)

Fig. 2. Received power at tag (modelled) vs. distance between reader and tag antennas for the free space, two- and three-ray models. hrd = 1.23m; htag = 0.265m; hc = 3.19m. Relative permittivities of floor (εrf) and ceiling (εrc): (a) 2 and 3, (b) 12 and 3, (c) 12 and 10.

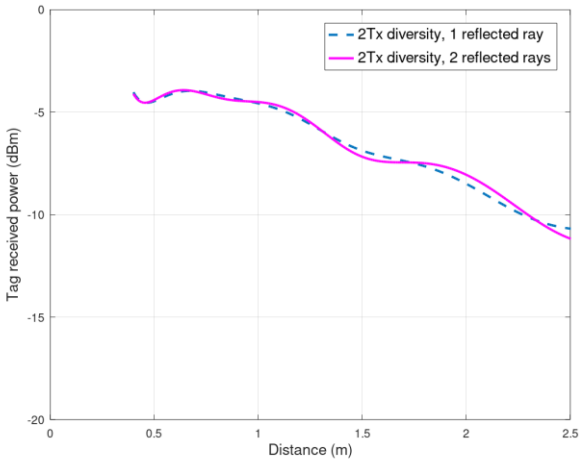

Fig. 3. Received power at tag vs. distance between reader and tag antennas for the multi-LOS multi-ray reflection model of (3). hrd1 = htag = 1.23m; hrd2 = 0.85m; hc = 3.19m; εrf = 2.

III. EXPERIMENTAL SETUPS

In this work, the IDS evaluation board model DK-R902-LP2 is used as RFID reader. It supports the Electronic Product Code Generation 2 (EPC Gen 2) protocol and has a receiver sensitivity of -59 dBm and nominal output power of +23 dBm. This reader uses a single port to connect to a vertically-polarized ceramic patch antenna. However, for the experiments reported here, two or three circularly-polarized antennas, model Favite FS-GA204, are employed instead of the original antenna. The single port RFID reader is connected to the Tx and Rx antennas via a circulator (Wenteg Microwave F2567-0089-15). The use of separate antennas improves the isolation between the Tx and Rx channels in comparison with a single antenna configuration. The reader is set to amplitude-shift keying (ASK) modulation, Miller 4 coding, and a Type-A reference interval (Tari) of 25 µs. The experiments were carried out at the central frequency of 865.7 MHz. A passive Smartrack tag (model DogBone–Impinj Monza R6) with a sensitivity of -20 dBm and positioned for horizontal polarization is used. Measurements with another tag (AMS SL900A) were also carried out with short range obtained due to the poor tag sensitivity. In this paper, only the results for the Smartrack tag are included.

In a first experiment, the received power levels (at the RFID reader) and tag read counts for either transmit or receive (spatial) antenna diversity in the vertical direction are measured and compared with the performance results for a no diversity case (1Tx-1Rx antennas). The transmitted power (at the Tx antenna input) is +21.2 dBm for the 1Tx-1Rx case. In Fig. 4, the antenna setup for the transmit diversity experiment is presented. The two transmit antennas are connected to the circulator and reader output through a RF splitter and short RF cables. The transmit power at each antenna input is reduced by 3 dB, which gives the same total transmit power as for the no antenna diversity case. For the receive diversity experiment, the lower Tx antenna in Fig. 4 was converted to a Rx antenna by connecting it to the Rx port of the circulator via a RF combiner. For the no diversity case, the lower Tx antenna in Fig. 4 was removed. The antenna separation of 12 cm was chosen based on a preliminary test in which a higher received power level was obtained for this separation (between Tx and Rx reader antennas) in comparison with greater separations.

The antenna setup for another experiment considering the effect on tag detection of placing a metallic (aluminum) plate near the tag is shown in Fig. 5. In this case, the center of the tag is at 26.5 cm above the floor and the received power level (at the reader) is measured with and without the aluminium plate. The dimensions of the aluminium plate are 27.5 x 43 x 0.5 cm and it is placed horizontally at 2.8 cm above the floor.

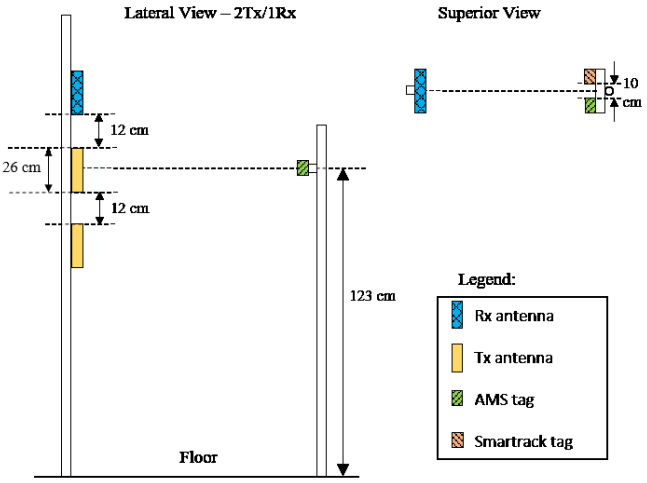

Fig. 4. Antenna setup for the transmit diversity experiments.

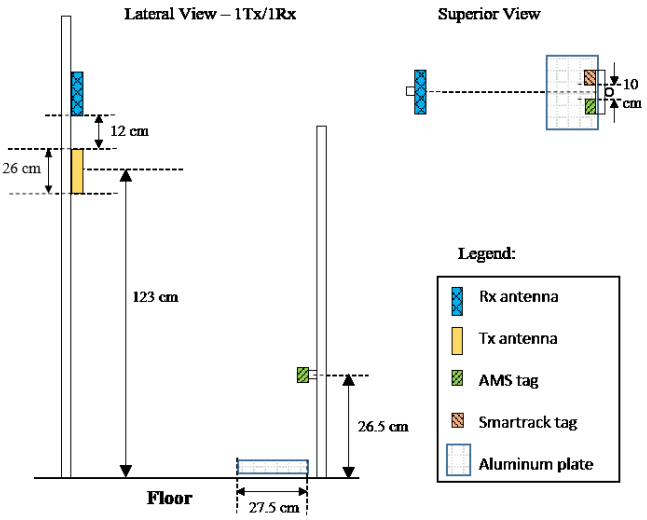

Fig. 5. Antenna setup for the experiment with the metallic plate.

IV. Experimental Results

A. Antenna Diversity Experiments

The received power levels at the RFID reader for the three antenna configuration schemes are shown in Fig. 6. The readings are taken at 20 cm steps, from 20 cm distance up to 80 cm, and in 10 cm steps beyond this. We stopped the measurements at 250 cm as no significant difference between the two diversity cases was found beyond 230 cm and also to avoid a possible strong interference from a wall in the laboratory. From Fig. 6, it can be seen that the best performance is obtained with the receive diversity scheme. At the tag-reader distance of 220 cm, for example, the received power level is higher than that of the no antenna diversity case by around 9.5 dB and 7.5 dB for the receive and transmit antenna diversity cases, respectively. As shown in Fig. 7, better tag read count is achieved with the receive diversity compared to the no antenna diversity case, mainly at longer distances. Up to the distance of 220 cm, the tag read count of the transmit diversity case was also better than that of the single antenna case (not plotted in Fig. 6 for clarity). By comparing Figs. 6 and 7, it can be seen that there is a good correlation between the power level dips and the dips in the read count (although not for every single point).

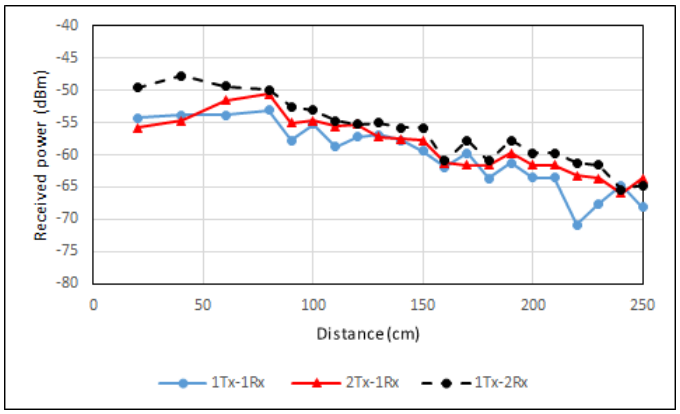

Fig. 6. Received power level (at reader) as a function of tag distance. No antenna diversity (1Tx-1Rx), transmit antenna diversity (2Tx-1Rx), and receive antenna diversity (1Tx-2Rx) schemes.

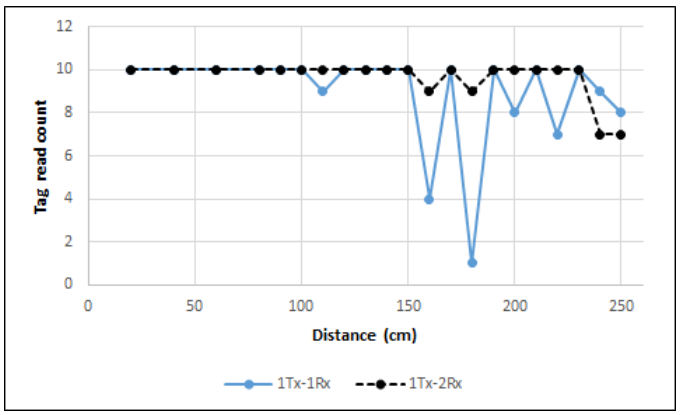

Fig. 7. Tag read count as a function of tag distance.

B. Experiments with a metallic plate in front of the tag

The experimental results for the setup of Fig. 5 are presented in Fig. 8. The readings are taken at 20 cm steps, from 2 m distance up to 7.4 m. From Fig. 8, it can be seen that the tag reading improves significantly by placing the aluminum plate on the ground in front of the tag. Without the aluminum plate there is no tag detection below 3 m distance and many null (no reading) points occur beyond this. With the aluminum plate, the tag is readable between 2 and almost 7 m, with just one null at 6.2 m. Apart from this null, the received power is always higher for the aluminum plate case. For example, the difference is about 8 dB at the distance of 3 m. The better performance obtained with the aluminum plate can be

explained with the aid of geometrical optics theory. As the tag antenna height is much lower than the reader Tx antenna, part of the backscattered waves from the tag move towards the floor. The aluminum plate reflects these waves towards the Rx antenna, which was placed even higher than the Tx antenna (see Fig. 5). Another reason is that the aluminum plate increases the amount of RF energy (from the reader antenna) harvested by the tag. This was observed in a previous experiment (with another aluminum plate) when the received power at tag location was measured with a spectrum analyzer.

As predicted by the three-ray model (Fig. 2), there are peaks in the experimental results of Fig. 8 after 3-m distance for both with and without metallic plate. Thus, both experiments are better modelled by the three-ray model.

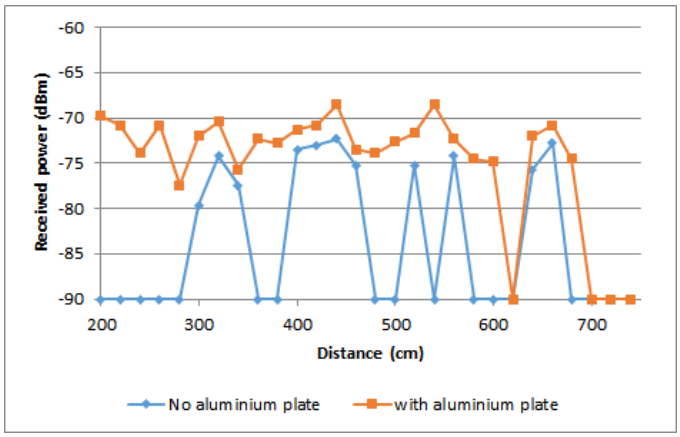

Fig. 8. Received power level (at reader) as a function of tag distance, with/without the aluminum plate below the tag. The -90 dBm power level just represents nulls (no reading).

V. CONCLUSION

In this work, analytical and experimental results considering the effects of indoor wave propagation and antenna diversity have been presented for passive UHF RFID systems. The tag received power level is simulated by using the two-ray and three-ray models, with the effect of changing relative permittivity of floor and ceiling discussed. In comparison with the experimental data, a better modelling is obtained with the three-ray model. In addition, the multi-LOS multi-ray reflection model has been proposed with good results reported. However, further model validations are still necessary considering other multiple antenna cases.

Experimental results for simple antenna receive or transmit diversity approaches are reported and compared with a no diversity case. The best performance, in terms of received power level and tag read count, is obtained with the receive diversity scheme.

In another experiment, without antenna diversity, promising performance improvement in the tag readability is demonstrated by simply placing an aluminium plate on the floor nearby a commercial tag.

As future work, changes in the metallic plate dimensions and its position in relation to the tag can be investigated. In addition, other antenna setups and diversity schemes can be investigated.

REFERENCES

[1] K. Finkenzeller, *RFID Handbook: Fundamentals and Applications in Contactless Smart Cards, Radio Frequency Identification and Near-Field Communication,* 3rd ed. Wiley & Sons Ltd., Chichester, UK, 2010.

[2] S. Sabesan, M. J. Crisp, R. V. Penty and I. H. White, "Wide Area Passive UHF RFID System Using Antenna Diversity Combined with Phase and Frequency Hopping," in *IEEE Transactions on Antennas and Propagation*, vol. 62, no. 2, pp. 878-888, Feb. 2014.

[3] R. Langwieser, C. Angerer, and A. L. Scholtz, "A UHF Frontend for MIMO Applications in RFID", in *IEEE Radio and Wireless Symposium*, New Orleans, USA, January 2010.

[4] T. S. Rappaport, *Wireless Communications: Principles and Practice* (2nd ed.), Prentice Hall PTR, Upper Saddle River, NJ, USA, 2002.

[5] P. V. Nikitin, K. V. S. Rao, S. F. Lam, V. Pillai, R. Martinez, and H. Heinrich, "Power Reflection Coefficient Analysis for Complex Impedances in RFID Tag Design," *IEEE Trans. Microw. Theory Tech.*, vol. 53, no. 9, pp. 2721–2725, Sep. 2005.

[6] M. Omer, G. Y. Tian, "Indoor Distance Estimation for Passive UHF RFID Tag Based on RSSI and RCS", *Measurement*, vol. 127, pp. 425-430, 2018.

[7] A. Lazaro, D. Girbau, and D. Salinas, "Radio Link Budgets for UHF RFID on Multipath Environments," *IEEE Transactions on Antennas and Propagation*, vol. 57, no. 4, pp. 1241-1251, Apr. 2009.

[8] A. A. Goes, P. Cardieri, and M. D. Yacoub, "Characterization of the RFID Deterministic Path Loss in Manufacturing Environments," *2012 IEEE 23rd International Symposium on Personal, Indoor and Mobile Radio Communications - (PIMRC)*, Sydney, NSW, pp. 647-652, 2012.

[9] L. C. Vieira, N. J. Gomes, J. C. Batchelor, A. Nkansah, P. Assimakopoulos, and M. A. Ziai, "RFID over Low Cost VCSEL-based MMF Links: Experimental Demonstration and Distortion Study," *IET Optoelectronics*, 2019. (Revised and resubmitted)

[10] Y. He and Z. Pan, "Design of UHF RFID Broadband Anti-Metal Tag Antenna Applied on Surface of Metallic Objects," in *Proc. IEEE Wireless Commun. Netw. Conf. (WCNC'13)*, pp. 4352–4357, 2013.

[11] H. D. Chen and Y. H. Tsao, "Broadband Capacitively Coupled Patch Antenna for RFID Tag Mountable on Metallic Objects," *IEEE Antennas Wireless Propag. Lett.*, vol. 9, pp. 489–492, Jun. 7, 2010.

[12] Y. Lin, M. Chang, H. Chen, and B. Lai, "Gain Enhancement of Ground Radiation Antenna for RFID Tag Mounted on Metallic Plane," in *IEEE Transactions on Antennas and Propagation*, vol. 64, no. 4, pp. 1193-1200, April 2016.

[13] A. Goldsmith, *Wireless Communications,* Cambridge University Press, 2005.